Journal of The Electrochemical Society, **149** (9) B422-B427 (2002)
0013-4651/2002/149(9)/B422/6/$7.00 © The Electrochemical Society, Inc.

Monitoring of Hydrogen Absorption into Titanium Using Resistometry

Kazuhisa Azumi,*,z Yoshihide Asada, Tomohiro Ueno, Masahiro Seo,* and Tadahiko Mizuno

Graduate School of Engineering, Hokkaido University, Kitaku, Sapporo 060-8628, Japan

Hydrogen absorption into Ti electrodes during electrochemical cathodic polarization was monitored using resistometry. Electric resistance of Ti increased with H absorption due to growth of a hydride layer from the surface toward the inside. The growth rate of the hydride layer was estimated from resistance data and was found to depend on the polarization current density, existence of a preformed anodic oxide film, and shape of the specimen. For example, preformation of an anodic oxide film at a potential higher than the breakdown potential, rather, promotes hydrogen penetration. In the case of a thin wire electrode, the hydride layer grew in a nonuniform manner because the volume expansion induced cracking on the surface. Therefore, the average thickness of the hydride layer was estimated from the change in resistance.
 [DOI: 10.1149/1.1498257]

Manuscript submitted August 6, 2001; revised manuscript received March 12, 2002. Available electronically July 29, 2002.

Titanium has strong corrosion-resistive properties, but it can be degraded by hydrogen absorption such as hydrogen embrittlement. Titanium absorbs a considerable amount of hydrogen and forms a hard and brittle Ti hydride phase, TiH_x, resulting in its structural failure. There have been many pioneering studies on physicochemical properties of a Ti/H system[1] and more practical studies in corrosion engineering areas such as hydrogen cracking of Ti.[2-5] These studies have shown that rates of hydrogen penetration, hydride growth, and crack formation are dependent on crystalline structure, mechanical stress, and rolling orientation. Not only cathodic polarization but also formation of galvanic coupling with other metals may cause hydrogen evolution on and its penetration into Ti. A surface oxide layer plays an important role in protecting a substrate Ti metal from corrosion (anodic dissolution) in an oxidative environment. However, under the condition of hydrogen evolution, hydrogen atoms can penetrate into the oxide layer, causing the transformation of Ti oxide into hydroxide,[6] and finally reach the substrate Ti. Recently, Ti has been considered as a candidate material for a container and related components for high-radiation-level nuclear waste.[7,8] Therefore, development of a technique for *in situ* monitoring of hydrogen absorption into Ti is important for practical applications of Ti.

Resistometry has been used for *in situ* monitoring of corrosion of steel,[9,10] for investigation of a passive film on iron,[11,12] and for investigation of anodic dissolution and pitting of iron.[13] In this technique, change in electric resistance (R) is connected with shrinking of electrodes due to corrosion loss or to change in electric properties of materials due to composition changes. Resistometry is also used for evaluation of hydrogen content in Pd because R depends on the atomic ratio, H/Pd.[14] It has also been reported that the resistance of Ti changes with hydrogen content.[15-18] The electric conductivity of a Ti hydride is considerably lower than that of a Ti metal. The aim of the present study was, therefore, to examine the applicability of resistometry to an *in situ* technique for monitoring hydrogen absorption into Ti. R was monitored during cathodic polarization for hydrogen absorption into a Ti electrode with a small cross-sectional area. From the resistance data, growth of the hydride layer was analyzed.

Experimental

The experimental setup was described in a previous paper.[13] Several kinds of Ti specimens were examined. A typical working electrode (WE) was a Ti wire (Nilaco Co., 99.6% purity, 0.1 or 0.125 mm diam, and 100 mm long) in coiled form to reduce its apparent size. Ti foil (Nilaco Co., 99.5% purity, 1 mm wide, 10 mm long, and 0.05 mm thick) was also used. These specimens were rinsed in acetone using an ultrasonic cleaner before experiments, and two wires were attached at both ends for traditional four-wire resistance measurements. Electric junctions were covered with silicone sealant. Specimens were etched before experiments for *ca.* 2 s in 2.0 wt % HNO_3 and 1.2 wt % HF to remove the oxide layer, and immersed immediately in the experimental solution. The electrolyte solution was 0.05 mol dm^{-3} H_2SO_4 solution, prepared from analytical-grade chemicals and doubly distilled water, followed by purification using a Millipore Milli-Q purification system. A single bottle made of polyethylene was used as an electrochemical cell. The electrolyte solution was bubbled with nitrogen gas during the experiment. Ti wire electrodes were cathodically polarized to charge hydrogen at various current densities in the range -0.1 to -100 mA cm^{-2}. R

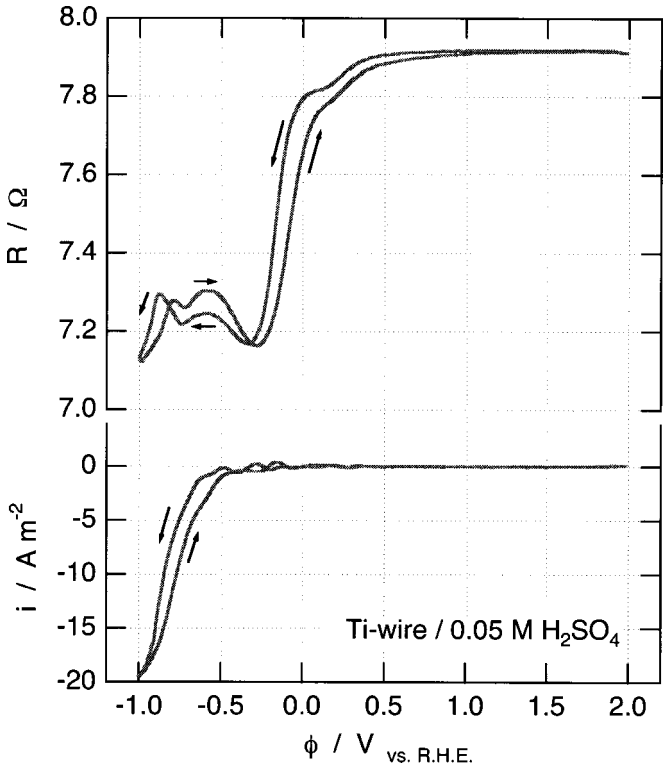

Figure 1. Changes in resistance, R, and polarization current, i_p, of Ti wire electrodes during a potential sweep in 0.05 mol dm^{-3} H_2SO_4 solution after 5 times potential sweeps.

* Electrochemical Society Active Member.
z E-mail: azumi@elechem1-mc.hokudai.ac.jp

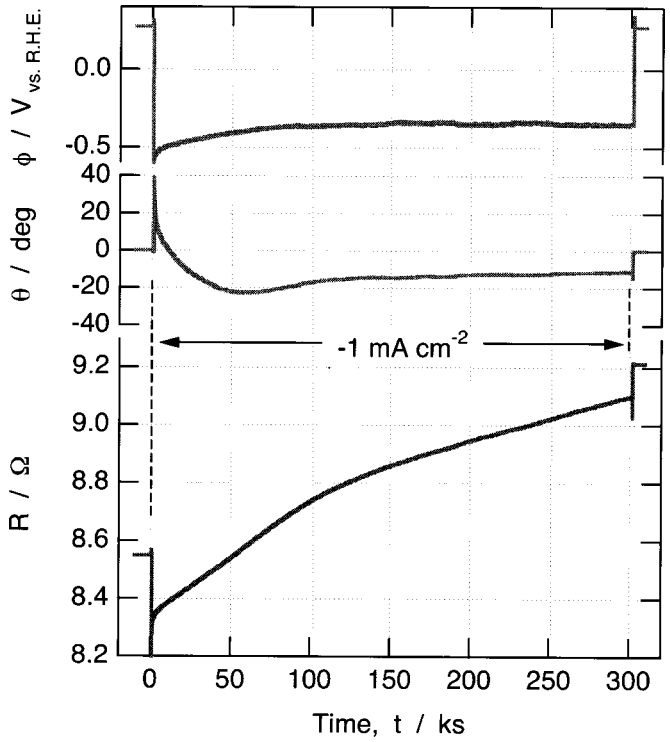

Figure 2. Changes in resistance, *R*, phase, θ, and electrode potential, ϕ, of Ti wire electrode during cathodic polarization at −1 mA cm^{-2} in 0.05 mol dm^{-3} H_2SO_4 solution.

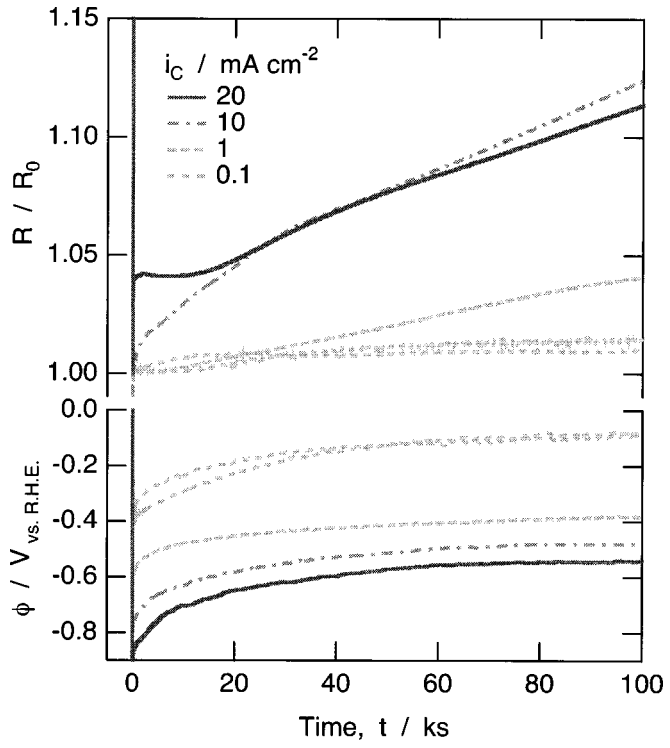

Figure 3. Changes in relative resistance, R/R_0, and electrode potential, ϕ, of Ti wire electrodes during cathodic polarization at various current densities in 0.05 mol dm^{-3} H_2SO_4 solution.

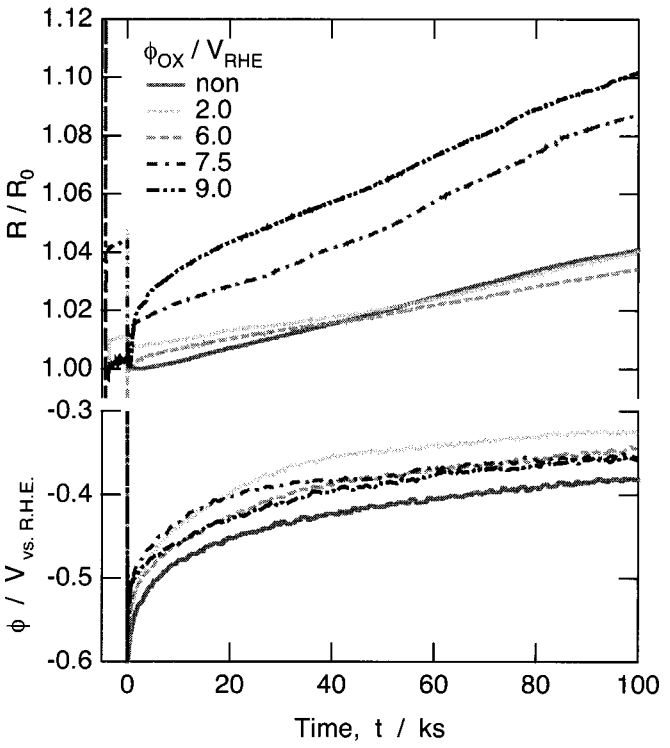

Figure 4. Changes in relative resistance, R/R_0, and electrode potential, ϕ, of Ti wire electrodes during cathodic polarization at −1 mA cm^{-2} in 0.05 mol dm^{-3} H_2SO_4 solution after preformation of an anodic oxide film at 2, 6, 7.5, and 9 V for 3.6 ks.

was measured using an ac technique in which a digital lock-in amplifier (DLA, N.F. Circuit Design, model LI5640) was used to apply an ac current (10 mA_{p-p}, 11 Hz) to the WE, and the resultant ac voltages on the WE and on a reference resistance connected serially to the WE were measured. At high frequency, *R* tends to decrease because the ac current leaks through the surface to the electrolyte

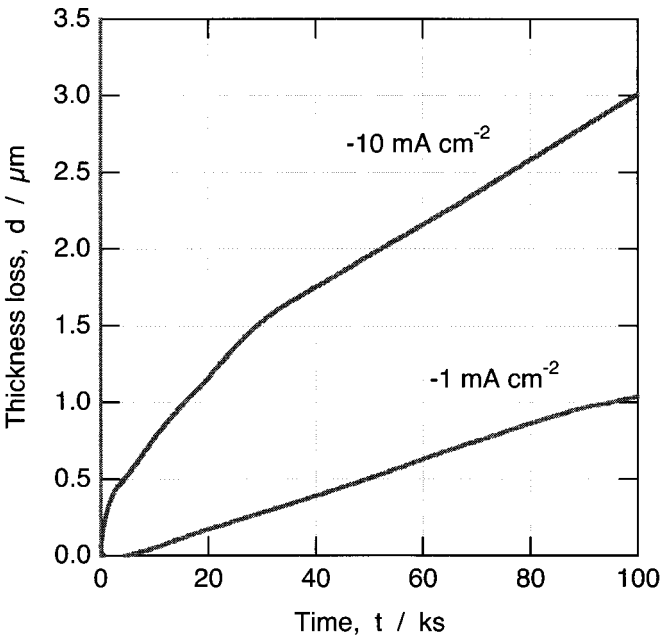

Figure 5. Time variation in thickness loss, *d*, of Ti due to growth of a TiH_x layer calculated from the data shown in Fig. 3.

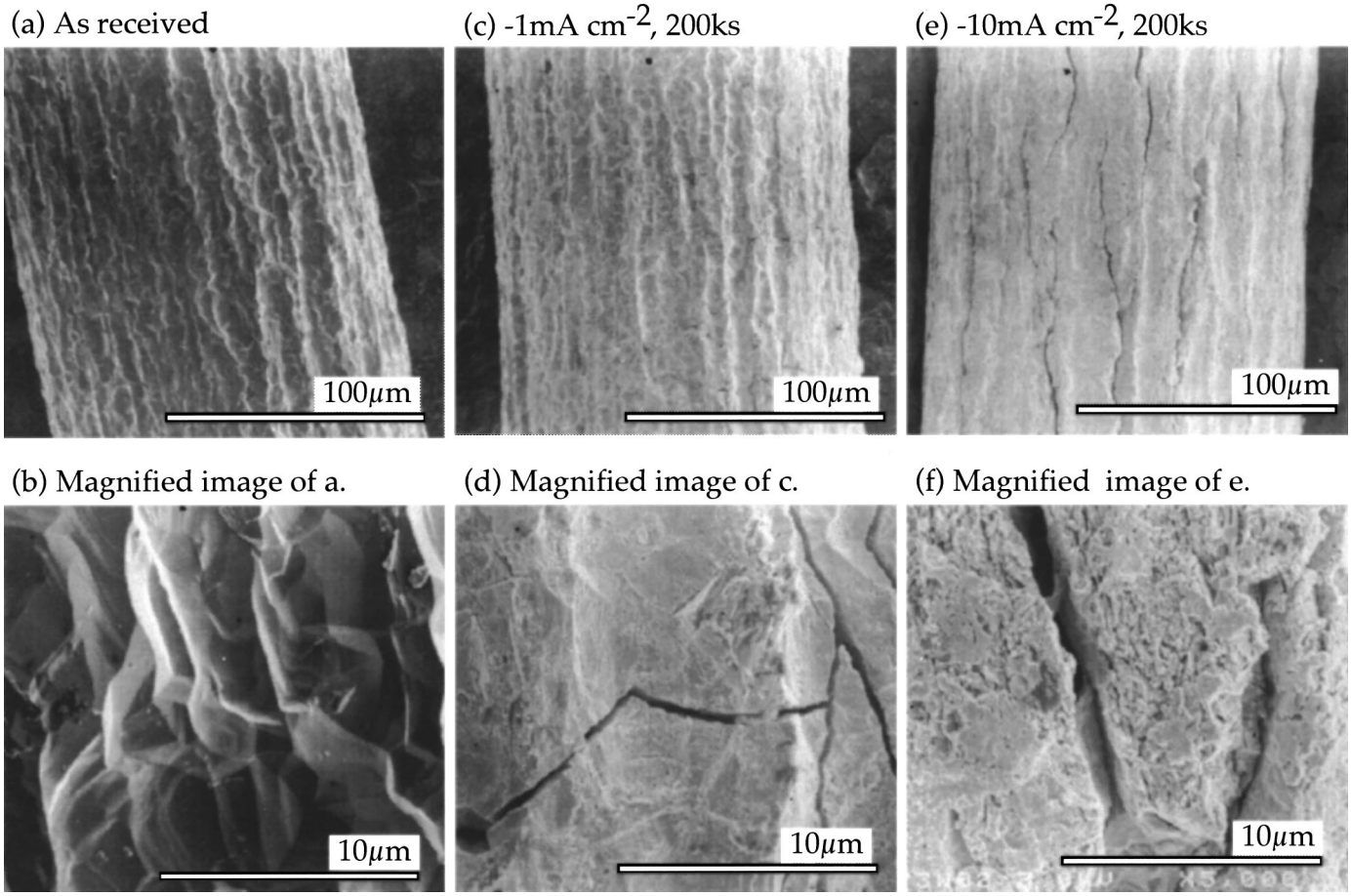

Figure 6. SEM images of a Ti wire of 125 μm diam with different magnifications (a, b) before and after cathodic polarization at (c, d) −1 or (e, f) −10 mA cm^{-2} for 200 ks in 0.05 mol dm^{-3} H_2SO_4 solution.

surrounding the WE. Resultant resistance is displayed as a relative resistance change, R/R_0, where R_0 is the lowest resistance that appeared in the initial stage of cathodic polarization, and R is resistance changing with hydrogen absorption. The actual resistance of the Ti wire electrode was about 8 Ω. A potentio/galvanostat (Nichia Co., model Tripot Potentio/galvanostat), a digital multimeter (Keithley, model 2000), and a water bath for controlling the temperature of the electrochemical cell were used for measurements. The whole system was controlled by a computer (Apple Computer Co., model PowerBook 180C) through a serial/GPIB interface. The morphology of the electrode surface was observed using a field-emission scanning electron microscope (FE-SEM, JEOL Co. model JSM-6300F), and the cross sections of the wire electrode were observed using a scanning confocal laser microscope (SCLM, Lasertech Co., model 1SA21).

Results and Discussion

Hydrogen absorption into Ti wire electrodes.—Figure 1 shows typical traces of resistance R and polarization current during a cyclic potential sweep, measured after potential sweeps for several times to obtain stable i-V curve. The surface was covered by anodic oxide film with ~6 nm thick.[19] R shows almost constant and relatively high values in the passive potential region higher than 0.5 V and lower values in the hydrogen evolution region lower than −0.3 V. In this study, change in R due to growth of the anodic oxide film was negligibly small compared with resistance change induced by hydride formation. In the potential region between 0.5 and −0.3 V, R decreases with decrease in potential. Under this condition, the space-charge layer in the n-type semiconductor oxide film disappears in the transition from an inverse bias condition at the noble potential to a noninverse bias condition at less-noble potential. Penetration of H atoms into the oxide film also raises the electric conductivity of the oxide film.[20] At a potential lower than −0.3 V, R shows a relatively low value because a part of the ac current applied to the wire electrode leaks through the electrically conductive surface to the electrolyte surrounding the wire electrode to reduce the apparent resistance.[13] Such a drop in R depends on the current density of cathodic polarization.

Figure 2 shows time variation of R during hydrogen absorption under the condition of galvanostatic polarization. In the initial stage of the experiment, R dropped when cathodic polarization started due to leakage of the ac current to the electrolyte as mentioned previously. When cathodic polarization was terminated R increased again. Therefore, the relative resistance change, R/R_0, where R_0 is the lowest value of R at the initial stage of hydrogen absorption, was used. However the influence of polarization current on resistance may induce some error to quantitative analysis described below. Figure 2 shows that R increased continuously during hydrogen absorption due to growth of the hydride layer. A considerable shift in phase θ during hydrogen absorption means a slow time response of resistance change against ac current perturbation. Change in the electrode potential shows that the overpotential for hydrogen evolution reaction becomes larger with increase in current density. In the initial stage, electrode potential shifted steeply in a less-noble direction, then shifted in a noble direction, and finally attained a steady state. Such behavior of the electrode potential of Ti during hydrogen absorption is not well understood.

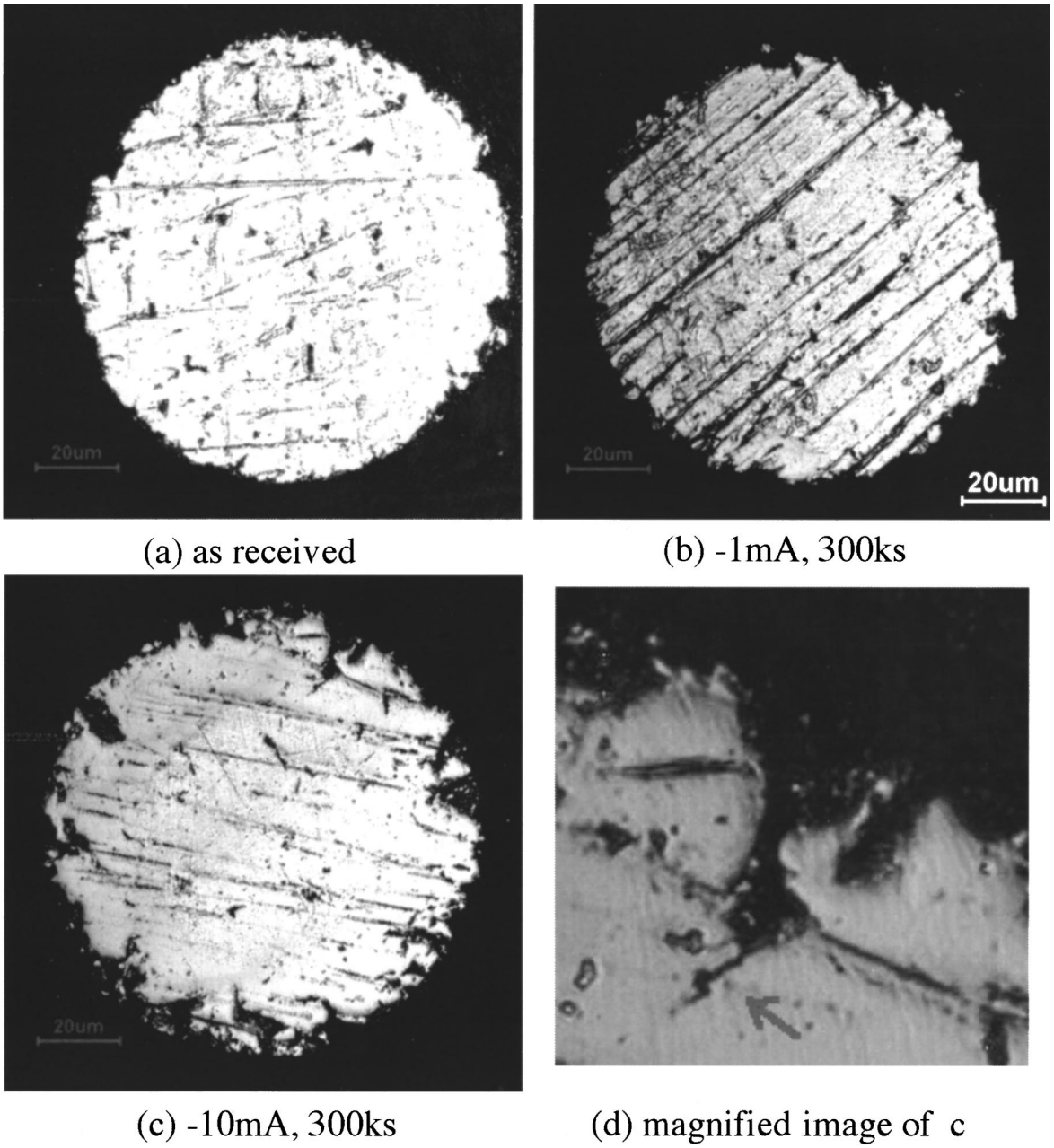

Figure 7. SCLM images of cross sections of Ti wire electrodes (a) before and after hydrogen absorption at (b) -1 and (c) -10 mA cm^{-2} for 300 ks in 0.5 mol dm^{-3} H_2SO_4 solution. (d) Magnified image of (c).

Figure 3 shows time variation of R/R_0 and electrode potential, ϕ, during hydrogen absorption at various cathodic current densities. R/R_0 increased immediately after the start of cathodic polarization, depending on the current density. A relatively rapid increase in R/R_0 means rapid growth of the hydride layer at larger current density.

It is expected that the surface oxide film on Ti prevents H penetration. The Ti wire electrode after etching pretreatment is immediately covered with a thin oxide film. For the formation of a thicker oxide film, the wire electrodes were potentiostatically polarized at various anodic potentials before hydrogen absorption. Figure 4 shows time variation of R/R_0 and potential during cathodic polarization of Ti electrodes covered with preformed anodic oxide films. The rates of increase in R/R_0 of specimens oxidized at 2 V (*ca.* 6 nm) and 6 V (*ca.* 15 nm) are almost same as that of a nonoxidized specimen, indicating that the anodic oxide layer does not prevent H penetration. For the specimens covered with thicker films formed at 7.5 V (*ca.* 18 nm) and 9 V (*ca.* 28 nm), however, hydrogen absorption was rather accelerated. It has been reported that anodic oxide films formed at a potential higher than 7.5 V are subjected to breakdown caused by microcrystallization of the oxide film due to a very high electric field,[19] resulting in an increase of film thickness and surface roughness,[21] especially in a sulfuric acid solution.[22] Progress of microcrystallization increases the surface roughness, *i.e.*, increase in surface area, which may promote efficient hydrogen absorption. Transformation of the film structure from amorphous at a lower potential to microcrystalline at a higher potential may also produce a pathway for H transfer via grain boundaries. Overpotential of the hydrogen evolution reaction on electrodes covered with preformed anodic oxide film is less than that on electrodes without preoxidation pretreatment. The surface of the anodic oxide film is probably hydrated, making hydrogen penetration easier than that in the case of an the air-formed oxide film. After penetration of hydrogen atoms

into the anodic oxide film, its structure changes gradually from TiO_2 to TiOOH.[6]

Ti hydride (TiH_x) forms an α-phase (fcc + hcp, face-centered cubic and hexagonal close-packed, lattice constant LC = 4.41 Å for fcc) at $X < 1.45$, γ-phase (fcc, LC = 4.42 Å) at $X < 1.71$, and ϵ-phase (fcc, LC = 4.44 Å).[23] Electric resistivity also changes with hydrogen content, *i.e.*, it increases from 4.78×10^{-3} Ω cm (298 K) at $X = 0$ to 120×10^{-3} Ω cm (298 K) at $X = 1.86$ and then decreases to 70×10^{-3} Ω cm (298 K) at $X = 1.98$ with increase in hydrogen content.[15,16] The depth profile of H concentration in Ti was previously reported by Mizuno *et al.* as a function of current density and polarization time using the etching method.[24] They showed that the hydrogen absorption process can be divided into three stages. In the first stage, the rate of absorption is rather slow because hydrogen absorption is suppressed by the oxide layer. In the second stage, hydrogen content increases linearly with growth of hydride. In the third stage, hydrogen content increases in a parabolic or logarithmic manner because the surface layer of hydride with very high hydrogen content acts as a diffusion-limiting layer. A hydride layer with a dendrite structure grows toward the substrate metal. Therefore, the interface region between the hydride and substrate Ti is not smooth and, thus, the interface is not clearly defined. The electric resistance of TiH_x is considerably larger than that of metallic Ti as mentioned above. The average thickness of the TiH_x layer is estimated from the resistance data shown in Fig. 3, assuming that the electric conductance of Ti hydride is negligible compared with that of metallic Ti

$$\frac{R}{R_0} = \frac{1/A}{1/A_0} = \frac{\pi r^2}{\pi(r-d)^2} \rightarrow d = r\left(1 - \sqrt{\frac{R_0}{R}}\right) \qquad [1]$$

where A is the cross-sectional area, r is the radius of wire electrode, d is the thickness loss of Ti due to growth of an insulative TiH_x layer, and subscript 0 is assigned to the initial value before hydrogen absorption. In Fig. 5, growth of hydride layer estimated from resistance change during hydrogen absorption at −1 and −10 mA cm^{-2} is shown. In the case of −1 mA cm^{-2}, d increases almost linearly with polarization time. In the case of −10 mA cm^{-2}, growth kinetics of TiH_x is composed of multistages. However such multistage behavior was not reproducible because the hydride grew nonuniformly due to hydrogen cracking, as mentioned later.

Figure 6 shows FE-SEM images of Ti wire electrodes after experiments. After hydrogen absorption at −1 mA cm^{-2} for 200 ks (Fig. 6c and d), many cracks were found on the surface. In the case of −10 mA cm^{-2} (Fig. 6e and f), widened cracks and porous surface indicate further hydride growth.[23] Since no cracks were observed in the case of a Ti sheet specimen after H absorption in the same conditions, the cracks on the Ti wire electrode were thought to have been formed due to stress around a circumference caused by volume expansion of TiH_x. Such stress probably causes cracks to form along the vertical axis, as seen in the figures. Once a crack has formed, a new surface of the metallic Ti is exposed to the electrolyte, and this promotes the penetration of hydrogen evolved on the electrode to form further Ti hydride.

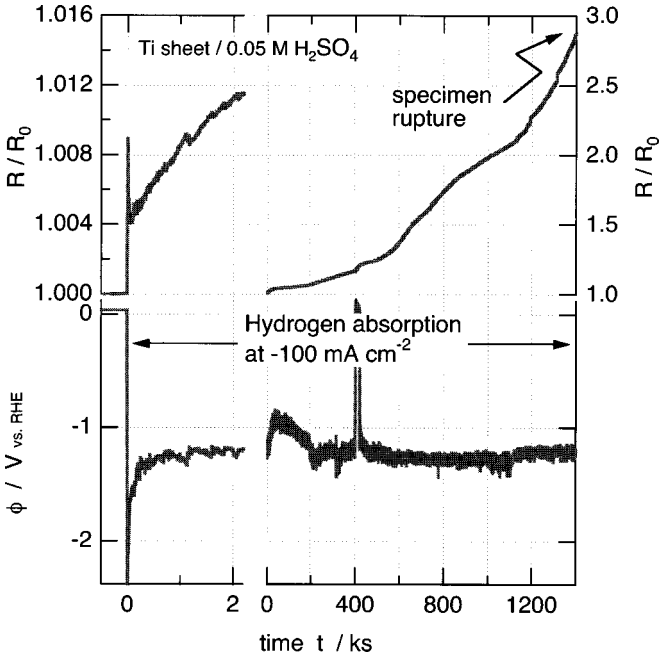

Figure 8. Changes in relative resistance, R/R_0, and electrode potential, ϕ, of a Ti sheet 50 μm thick and 1 mm wide during cathodic polarization at −100 mA cm^{-2} in 0.05 mol dm^{-3} H_2SO_4 solution.

Figure 7 shows cross-sectional images of Ti wire electrodes measured by SCLM after the experiment. These images indicate that a hydride layer grows in a nonuniform manner on the wire electrodes. A comparison of the magnified image shown in Fig. 7d with the surface images shown in Fig. 6 indicate that the crevices formed on the surface promoted the penetration of hydrogen to the deep location, formation of hydride there, and expansion of crevices with large stress due to volume expansion. Therefore, the thickness loss shown in Fig. 5 corresponds to an average value. It is clear that such effects are preferred for the wire-form specimen. In the case of a Ti plate, growth of a hydride layer through the dendrite formation proceeds uniformly from the surface and does not form any apparent cracks under the similar polarization condition for hydrogen absorption of Fig. 6.[23]

Heavy hydrogen charging into Ti foil electrodes.—Figure 8 shows the changes in R/R_0 measured for a Ti foil electrode during

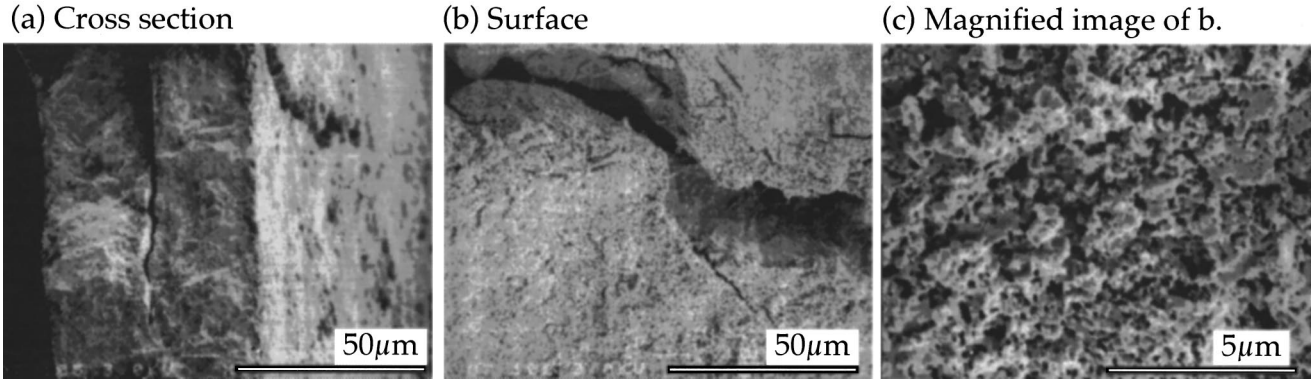

Figure 9. SEM image of a Ti foil (a) side and (b, c) front surfaces after cathodic polarization at −100 mA cm^{-2} for 1400 ks in 0.05 mol dm^{-3} H_2SO_4 solution.

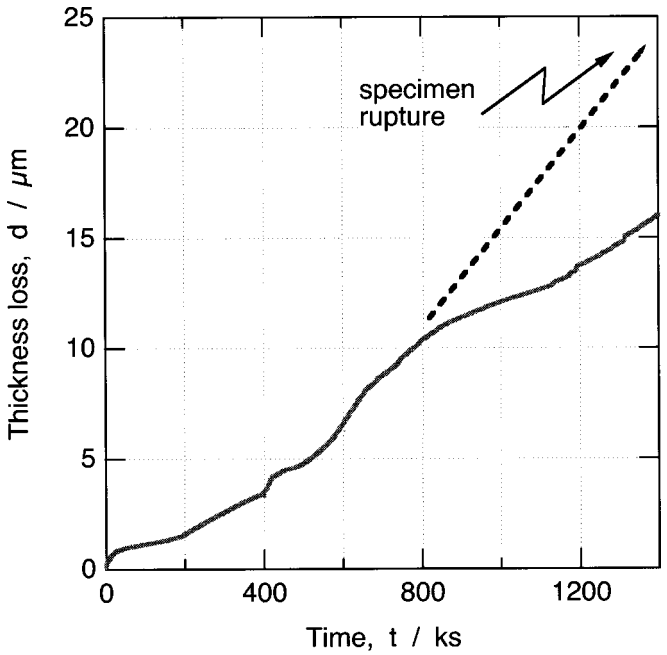

Figure 10. Time variation in thickness loss, *d*, of Ti due to growth of a TiH_x layer calculated from the data shown in Fig. 8.

hydrogen absorption at -100 mA cm^{-2} for a long period. R/R_0 increased considerably due to a large amount of H absorption. R/R_0 increased more steeply after 200 ks and reached almost 3 at 1400 ks, when the electrode was broken by hydrogen cracking.

Figure 9 shows FE-SEM images of the side and the front surfaces of a specimen after the experiment. A crack can be seen in the center of the side surface, indicating that large stress was applied from both faces of the specimen due to hydride growth. A crack can also be seen on the front surface. A magnified image (Fig. 9c) shows that the structure of the hydride is porous. Such structural change also affects the electric resistance of the electrode, and thus estimation of the thickness of the hydride layer seems difficult. In Fig. 10, thickness loss of metallic Ti calculated from the data in Fig. 8 is plotted. At 1400 ks, *d* seems to reach almost 25 μm, *i.e.*, half of the specimen thickness, because it was broken. The relatively low value of *d* calculated from resistance at this point can probably be explained by the ionic conduction due to electrolyte filling pores in the porous hydride layer shown in Fig. 9c.

Conclusions

In the present work, change in electric resistance of a Ti electrode during H absorption by electrochemical cathodic polarization was monitored. Resistance increased continuously with H absorption due to growth of the hydride layer until its rupture caused by hydrogen cracking. Analysis of resistance data showed that the efficiency of hydrogen absorption is influenced by the current density, surface conditions such as chemical etching pretreatment, properties of the surface oxide film, and the shape of the electrode. To estimate the thickness of the hydride layer from resistance data, leakage of the ac current for resistance measurement to electrolyte surrounding the electrode and other factors such as the porous structure of the hydride layer under heavy hydrogen absorption have to be considered. In the case of a wire-form specimen, the hydride layer grows nonuniformly due to hydrogen cracking, and the thickness of the hydride layer calculated from resistance data therefore corresponds to an average value. In conclusion, the resistometry technique is useful for *in situ* monitoring of hydrogen absorption into Ti in certain environments.

Hokkaido University assisted in meeting the publication costs of this article.

References

1. W. M. Mueller, in *Metal Hydrides*, W. M. Mueller, J. P. Blackledge, and G. G. Libowitz, Editors, Chap. 8, Academic Press, New York (1968).
2. D. G. Kolman and J. R. Scully, *Metall. Mater. Trans. A*, **28**, 2645 (1997).
3. M. A. Gaudett and J. R. Scully, *Scr. Mater.*, **36**, 565 (1997).
4. M. A. Gaudett and J. R. Scully, *Metall. Mater. Trans. A*, **30**, 65 (1999).
5. C. F. Clarke, D. Hardie, and B. M. Ikeda, *Corros. Sci.*, **39**, 1545 (1997).
6. T. Ohtsuka, M. Masuda, and N. Sato, *J. Electrochem. Soc.*, **134**, 2406 (1987).
7. A. Michaelis, S. Kudelka, and J. W. Schultze, *Electrochim. Acta*, **43**, 119 (1998).
8. D. B. Bullen, A. A. Sagues, P. P. Craig, C. A. W. Di Bella, and K. D. Severson, *J. Met.*, **52**, 30 (2000).
9. A. F. Denzine and M. S. Reading, *Mater. Perf.*, **37**, 35 (1988).
10. P. A. Cella and S. R. Taylor, *Corrosion (Houston)*, **56**, 951 (2000).
11. S. Haruyama and T. Tsuru, *Corros. Sci.*, **13**, 275 (1973).
12. T. Tsuru and S. Haruyama, *Corros. Sci.*, **16**, 623 (1976).
13. K. Azumi, K. Iokibe, T. Ueno, and M. Seo, *Corros. Sci.*, **44**, 1329 (2002).
14. T. Mizuno and M. Enyo, in *Modern Aspects of Electrochemistry*, R. E. White, B. E. Conwey, J. O'M Bockris, Editors, Vol. 30, pp. 415–503, Plenum Press, New York (1996).
15. M. M. Antonova, *OR: Svoistva Gidridov Metallov: Spravochnik*, Nissotuuhinsya, Kyoto (1976).
16. K. Gesi and Y. Takagi, *J. Phys. Soc. Jpn.*, **18**, 306 (1963).
17. N. E. Paton, B. S. Hickman, and D. H. Leslie, *Metall. Trans.*, **2**, 2793 (1971).
18. S. V. Ariyaratnam, N. A. Suplise, and E. H. Adem, *J. Mater. Sci. Lett.*, **6**, 1349 (1987).
19. T. Ohtsuka, M. Masuda, and N. Sato, *J. Electrochem. Soc.*, **132**, 787 (1985).
20. K. Azumi and M. Seo, *Corros. Sci.*, **43**, 533 (2001).
21. K. Azumi and M. Seo, *Hyomen-gijutsu*, **49**, 39 (1998).
22. K. Azumi, N. Yasui and M. Seo, in *Passivity and Localized Corrosion*, M. Seo, B. MacDougall, H. Takahashi, and R. G. Kelly, Editors, PV 99-27, pp. 215-224, The Electrochemical Society Proceedings Series, Pennington, NJ (2000).
23. T. Mizuno and M. Enyo, *Denki Kagaku oyobi Kogyo Butsuri Kagaku*, **63**, 719 (1995).
24. T. Mizuno, T. Shindo, and T. Morozumi, *Boshoku Gijutsu*, **26**, 185 (1977).